

A Model to Evaluate the Transient Hydraulic Response of Three-Dimensional Sparsely Fractured Rock Masses

DEREK ELSWORTH

Department of Mineral Engineering, Pennsylvania State University, University Park

A numerical model is presented for the analysis of transient fluid flow in large systems of rigid fissure discs. A boundary element procedure is invoked to minimize the number of equations required to define the system. Condensation of the system of equations at an elemental or individual disc level is used to cast the solution into finite element format. The resulting global matrices are well conditioned, sparsely populated, and apparently symmetric. The formulation is illustrated to perform well in validation studies for both single unconnected and multiply connected fissures. The procedure is ideally suited to the analysis of large, formerly intractable, fissure networks where the system degrees of freedom may be reduced to and retained at a minimum.

INTRODUCTION

The utilization of sparsely fractured rock masses as a potential host for highly toxic wastes has highlighted the inability of current characterization methods to describe adequately the hydraulic response. To date, groundwater hydrogeologists have been concerned primarily with aquifers of high yield where existing continuum and dual porosity models are found to perform adequately [Barenblatt *et al.*, 1960; Snow, 1966]. In sparsely fractured formations, however, these models are markedly deficient, and alternative treatment of the problem is required [Sagar and Runchal, 1982]. Use of discontinuum models incorporating discrete fractures is plagued with problems related to both the validity and quality of input data and the computational effort required to evaluate responses for even relatively modest realizations of fracture density [Noorishad *et al.*, 1982]. The development of simulation techniques capable of treating such problems on a routine basis is necessary to enhance a fundamental understanding of the physical interaction of components constituting such a system. Numerical simulation techniques provide a viable technique for investigating the fundamental phenomenological behavior of three-dimensional fractured rock masses in both steady and transient states. Only with the advent of this facility will improved predictions of the ultra-long-term performance of such systems help to contribute to successful waste immobilization.

It is evident that rock masses containing low densities of interconnected fractures may, in some instances, never reach the required "representative elemental volume" necessary to allow characterization as a continuum. This factor has been observed for steady flow in two-dimensional fracture networks [Long and Witherspoon, 1985] and would likely be equally true for three-dimensional flows in both steady and transient domains. Indeed, for transient flow the problem is further compounded in that the volume affected by a significant hydraulic disturbance changes with time. Thus it is conceivable that a rock mass that behaves as a discontinuum in the short term may transform to continuum characterization as the zone of hydraulic disturbance migrates.

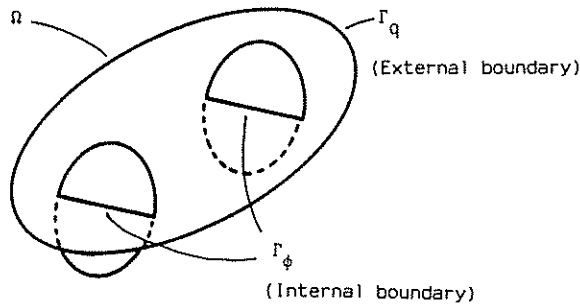
Routine site characterization and investigation using pumping tests may not be expected to yield useful results unless

appropriate forms of data reduction are invoked. Qualitative and quantitative analyses, in this regard, require an intimate appreciation of the discontinuous nature of the mass [Long, 1983]. The consequence of these factors is that under certain circumstances, continuum models may carry little validity and should therefore be used with extreme caution as a predictive tool.

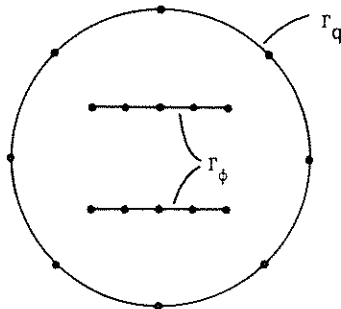
In addition to the geometric influence of the discontinuous fissures on the hydraulic performance of the rock mass, flow-related changes in effective stress may further affect flow patterns. Conventional tensorial representation of anisotropic aquifers cannot easily accommodate the consequences of shear-related dilational opening of rock fractures under changes in ambient effective stress. Changes in hydraulic conductivity and storage that result from modifications to fracture aperture may be extremely important [Elsworth and Goodman, 1985, 1986]. Similarly, the possibility of interconnection with superconducting joints and faults must not be overlooked. Incorporation of these factors into any analysis is only possible if discrete representation of individual fissures is possible.

The influence of all the factors mentioned above may be examined on a systematic basis for discretely fractured systems if efficient simulation techniques are available to provide appropriate sensitivity analyses. The complexity of the problem limits the applicability of analytical techniques in accurately representing global domain geometry and resulting performance. Although providing an invaluable and indispensable tool for validation, experimental and in situ characterization methods are difficult to justify on the basis of both their economy and the inherent difficulty in defining boundary conditions. This leaves numerical simulation techniques, by default, as potentially the most attractive contender.

From known statistical distributions of fissure aperture, density, trace length, and orientation, Monte Carlo techniques may be used to construct a representative rock mass as a series of Poisson discs. This aspect of the problem is fundamental in justifying the development and use of the simulation procedures reported in the following, although it is adequately covered in existing literature [Long, 1983]. No further discussion of statistical aspects will be made. To the assembled network, appropriate boundary conditions may be applied, and established numerical techniques may be used to predict steady state and transient response. Work in this vein has been completed for the steady analysis of two-dimensional



(a)



(b)

Fig. 1. (a) Three intersecting fissure discs and (b) representation of the central disc in boundary element format.

networks [Wilson and Witherspoon, 1974; Shapiro and Anderson, 1983] and preliminary reports for the three-dimensional steady problem made [Long et al., 1985; Elsworth, 1986]. The following presents a new approach to the steady problem and extends the capability into the transient domain.

A modified boundary integral method is presented to predict the transient performance of a single rigid fissure disc of constant aperture. Since the primary motivation is to be able to assemble a global system containing many tens or hundreds of such discs, it is essential that the number of nodal degrees of freedom per disc be reduced to a desired minimum.

NUMERICAL FORMULATION

Existing finite element, finite difference, and integrated finite difference solution techniques provide ready solution to the general diffusion problem. Adaptation to the specific problem of three-dimensional fissure flow is relatively straightforward, comprising in-fissure meshing of elements or nodes. Solution by finite element analysis yields generally well-conditioned, sparsely populated matrices of symmetric form. In all cases, however, the large number of nodes and the special meshing techniques required to provide reasonable nodal coverage within the plane of fissures for a typical problem are restrictive to implementation. Use of a boundary element formulation enables nodal coverage to be restricted to fissure edges and intersections only. Schematic representation of a system of three intersecting fissure discs is illustrated in Figure 1a together with a typical discretization of the central disc into boundary nodes and elements in Figure 1b. The nodes representing the fissure edges may be eliminated, as required, at the elemental level to leave a minimum of a single degree of freedom per intersection. For finite domains the resulting elemental matrices are, by inspection, symmetric and positive definite and may accommodate fissure geometries of arbitrary shape. All meshing and matrix reduction operations are performed at the local or elemental disc level prior to global matrix assembly. The technique is therefore ideally suited to microcomputer preprocessing and ultimate solution. Iso-parametric formulation may conveniently be implemented to represent accurately the curved outer boundaries of fissure discs, thus reducing to a minimum the number of nodes required to achieve a predefined level of precision.

Boundary Integral Equations

A single fissure disc of constant aperture may be represented as a planar flow domain Ω of area bounded by an edge contour Γ. Although the following application is made only to discs of circular edge contour, the formulation is entirely general and may accommodate equally domains of arbitrary shape. No particular computational advantage is reaped by assuming that the discs are circular. Where the external contour Γ encloses a homogeneous and isotropic domain Ω, the boundary constraint equation conforming to the direct formulation of the boundary element method may be stated as [Jaswon, 1963; Symm, 1963; Banerjee and Butterfield, 1981]

$$c(i)\phi(i) + \int_{\Gamma} V(i, j)\phi(j) d\Gamma = \int_{\Gamma} \Phi(i, j)v(j) \cdot \bar{n} d\Gamma \quad (1)$$

The kernel functions $V(i, j)$, and $\Phi(i, j)$ relate the radial

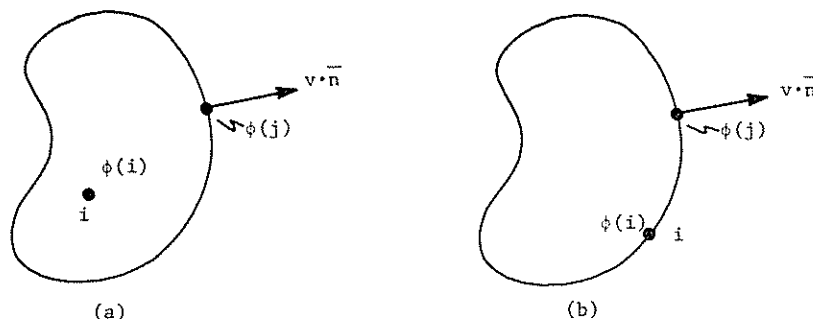


Fig. 2. Boundary element domain with source points placed (a) internally and (b) on the boundary.

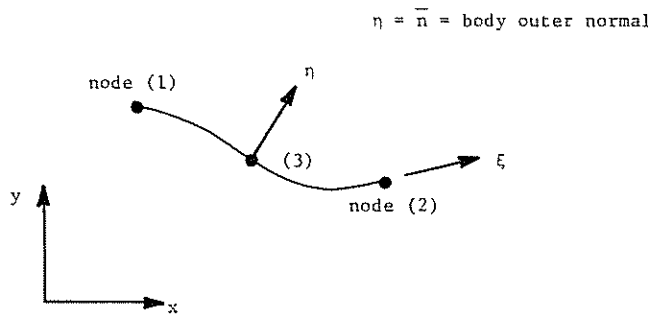


Fig. 3. The geometry of an isoparametric boundary element in two-dimensional space.

velocities and total hydraulic potential induced at point j due to a unit source at point i , respectively. The total hydraulic head and normal (to the boundary) velocity are defined as $\phi(j)$ and $v(j) \cdot \bar{n}$, respectively, where \bar{n} is the unit outward normal at j . The free term $c(i)$ is a function of the contour bounding the domain at the location of the imposed source i . Figure 2 illustrates two basic forms that the domain (Ω) may take. First (Figure 2a), the source i is located internally and the free term $c(i)$ is designated as equal to unity. If, as in Figure 2b, the source is brought to the domain boundary, the free term $c(i)$ is equal to one half if the external contour is smooth at i . The integration around the contour Γ implied in equation (1) yields a single equation where, for the case of the internal source illustrated in Figure 2a, the physical interpretation of the free term on the left-hand side is that the full influence of the source is retained within the domain. The equivalent statement for the boundary source of Figure 2b is that half of the influence is retained within the domain and half retained externally. In either case, the integration over the boundary of the terms in equation (1) will yield a single equation where i is the point of application of the source and j represents, in turn, all other line segments of differential length $d\Gamma$ along the boundary.

If the domain boundary Γ is divided into multiple "elements" of finite length, the source may be applied at designated points in each of the "elements" in turn and, for each application, a further boundary constraint relation will result. Thus for n "elements," n simultaneous equations will be produced. The format pursued in the following is to develop a node-centered system rather than an element-based system. Thus the influence of the source term at node i is evaluated over a tributary area at node j with recourse to consistent shape functions. Quadratic isoparametric representation is deemed most applicable in this instance to represent the truly curved nature of the contour boundary Γ .

Isoparametric Representation

A typical fissure disc discretized in boundary element form is illustrated in Figure 1b. Nodes located around the external and internal boundaries allow a single identity of type given in equation (1) to be written for each node. Appropriate kernel functions in this application are [Kellogg, 1953]

$$\Phi(i, j) = \frac{M}{2\pi} \ln r \tag{2a}$$

$$V(i, j)_r = -KM/2\pi r \tag{2b}$$

where K is the fissure hydraulic conductivity, r is the radius (i

to j), and the strength of the line source system is given by magnitude M . For laminar flow within a fissure of constant aperture the parallel plate analogy or any convenient modified form thereof may be used for K [Snow, 1966].

The boundary constraint equation (equation (1)) requires that integrations are completed along the contour of the domain boundaries Γ . It is most convenient to complete these integrations over the extent of the three-noded elements used in the formulation. Lagrangian basis functions may be used to relate nodal parameters of geometry (x, y), hydraulic head (ϕ), and normal to the boundary velocity ($v \cdot \bar{n}$) to values along the length of the element. The geometry of a single three-noded element is illustrated in Figure 3. The vector of basis functions is given as

$$\mathbf{h}^T = \frac{1}{2}[(1 - \xi) - (1 - \xi^2); (1 + \xi) - (1 - \xi^2); 2(1 - \xi^2)] \tag{3}$$

where $-1 < \xi < +1$ and ξ is the intrinsic coordinate along the length of the curved element. The values of any parameter may be expressed at any point within the element through the basis functions such that

$$x = \mathbf{h}^T \mathbf{x} \tag{4a}$$

$$y = \mathbf{h}^T \mathbf{y} \tag{4b}$$

$$\phi = \mathbf{h}^T \phi \tag{5a}$$

$$v \cdot \bar{n} = \mathbf{h}^T \mathbf{v} \cdot \mathbf{n} \tag{5b}$$

where the nonvectoral quantities (lightface) are defined at any point ξ by the nodal quantities (boldface) contained within respective three row vectors.

It is most convenient to evaluate the integrals of equation (1) in mapped form for each node on an element by element basis. Equation (1) may be rewritten in mapped form over the length of a single element as

$$c(i)\phi(i) + \int_{-1}^{+1} V(i, j)\phi(j) \frac{d\Gamma}{d\xi} d\xi = \int_{-1}^{+1} \Phi(i, j)v(j) \cdot \bar{n} \frac{d\Gamma}{d\xi} d\xi \tag{6}$$

where the Jacobian for the mapping is given as

$$d\Gamma/d\xi = [(dx/d\xi)^2 + (dy/d\xi)^2]^{1/2} \tag{7}$$

and appropriate substitution of equations (5a) and (5b) may be made into equation (6). The integrals must be evaluated over all elements composing the boundary to yield the equivalent of equation (1). The differentials comprising the Jacobian in equation (7) may be evaluated by differentiating the shape function vector \mathbf{h}^T of equation (3) such that

$$\frac{d}{d\xi} (\mathbf{x}) = \frac{d}{d\xi} (\mathbf{h}^T) \mathbf{x} \tag{8}$$

and similarly for y .

Integration of Kernel Functions

The integrals of equation (6) may, in almost all cases, be evaluated using Gaussian quadrature [Stroud and Secrest, 1966] along the length of the bi-unit element. To facilitate this, the Jacobian and unit normal vector must be evaluated at each of the Gauss points. Two-point quadrature has proved adequate in all instances to date. On two occasions, however, the integrals are unbounded as a result of singularities in the kernel terms of equation (2). These singularities occur when the node at which the source is applied coincides with the

node at which the influence is integrated (i.e., nodes i and j coincide). For the velocity kernel and free term on the left-hand side of equation (6) this problem is overcome by mass balance considerations. If the hydraulic head is everywhere set equal to unity ($\phi(j) = 1$), then by definition, the flow velocity on the boundary and everywhere within the domain must be identically zero. The right-hand side of equation (6) must therefore be zero for all nodes with the result that the influence at node $i = j$ is equal to the sum of all other integrals $j \neq i$. This is equivalent to requiring that the fluid volume exiting the domain over the tributary influence length of node i enters the domain over the scaled remainder of the contour length.

The singularity present in the potential kernel involves $\ln r$ and is unbounded when $i = j$ since $r \rightarrow 0$. This integral may be evaluated using a special logarithmic integration formula [Anderson, 1965] whereby

$$\int_0^1 f(x) \ln(x) \cong w_i f(x_i) \quad (9)$$

where w_i is an integration weight and $f(x_i)$ corresponds to the function evaluated at x_i . An appropriate change of variable is required for the integration to yield corrected limits between $+1$ and -1 .

Internal Slit Elements

The internal boundaries within fissure discs each represent a closed contour and may be treated in an identical manner to the external edge of the domain Ω . To maintain the number of degrees of freedom for an individual disc at a minimum, it is desirable to have individual slit elements capable of accommodating fluid flows from either side. In this manner it is not necessary to locate elements on both sides of what, in practice, is an infinitesimally thin slit. Recourse is made, therefore, to the fundamental definition of the boundary constraint equation (equation (1)) where the source term is contained entirely within the solution domain Ω . Thus where the equations are assembled for an internal source it is only the magnitude of the free term ($c(i)$) that differs from the equations developed where the source term is located on the external boundary. For sources enclosed entirely within the fissure disc the appropriate magnitude of the free term is δ_{ij} , where δ_{ij} is the Kronecker delta.

Matrix Assembly and Solution

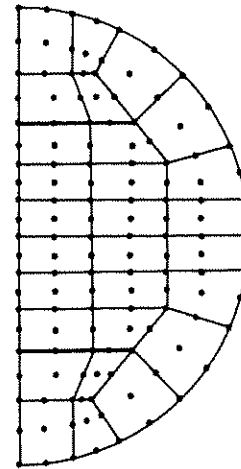
If n nodes are used to define the geometry of a single disc, a system of n simultaneous equations result. In matrix format these may be represented as

$$\mathbf{V}\phi = \Phi\mathbf{v} \quad (10)$$

where \mathbf{V} and Φ are fully populated square matrices of order n and ϕ and \mathbf{v} are vectors of nodal head and normal (to the boundary) velocity, respectively. A total of n boundary conditions must be prescribed in a well-posed problem to yield a solution to equation (10). If the matrix identity is subdivided according to boundary condition types, equation (10) may be rewritten as

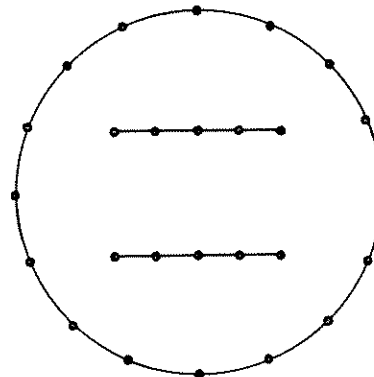
$$\begin{bmatrix} \mathbf{V}_{11} & \mathbf{V}_{12} \\ \mathbf{V}_{21} & \mathbf{V}_{22} \end{bmatrix} \begin{Bmatrix} \phi_1 \\ \phi_2 \end{Bmatrix} = \begin{bmatrix} \Phi_{11} & \Phi_{12} \\ \Phi_{21} & \Phi_{22} \end{bmatrix} \begin{Bmatrix} \mathbf{v}_1 \\ \mathbf{v}_2 \end{Bmatrix} \quad (11)$$

where boundary conditions may be set separately over segments 1 and 2 corresponding to the subscripts on the vector



(a)

• nodal points



(b)

Fig. 4. Equivalent (a) finite element and (b) boundary element discretizations used for validation.

quantities. Appropriate boundary conditions for the disc geometry are zero flow on the external edge, say segment 1, and as yet unknown heads on the internal slits comprising segment 2. Column substitution of equation (11) to render all known terms on the right-hand side yields

$$\begin{bmatrix} \mathbf{V}_{11} & -\Phi_{12} \\ \mathbf{V}_{21} & -\Phi_{22} \end{bmatrix} \begin{Bmatrix} \phi_1 \\ \mathbf{v}_2 \end{Bmatrix} = \begin{Bmatrix} -\mathbf{V}_{12} & \phi_2 \\ -\mathbf{V}_{22} & \phi_2 \end{Bmatrix} \quad (12)$$

since $\mathbf{v}_1 = 0$. Equation (12) may be solved for \mathbf{v}_2 if the distribution of potential on the internal boundaries ϕ_2 were known. Alternatively, the system of equations may be solved for a series of boundary condition cases prescribed by the user. Since the unknown boundary conditions are only present for the m nodes composing the internal slit elements, the right-hand side of equation (12) may be evaluated where an individual internal node is set to unit potential and all others ($m - 1$ nodes) retained at zero. If this procedure is completed for each

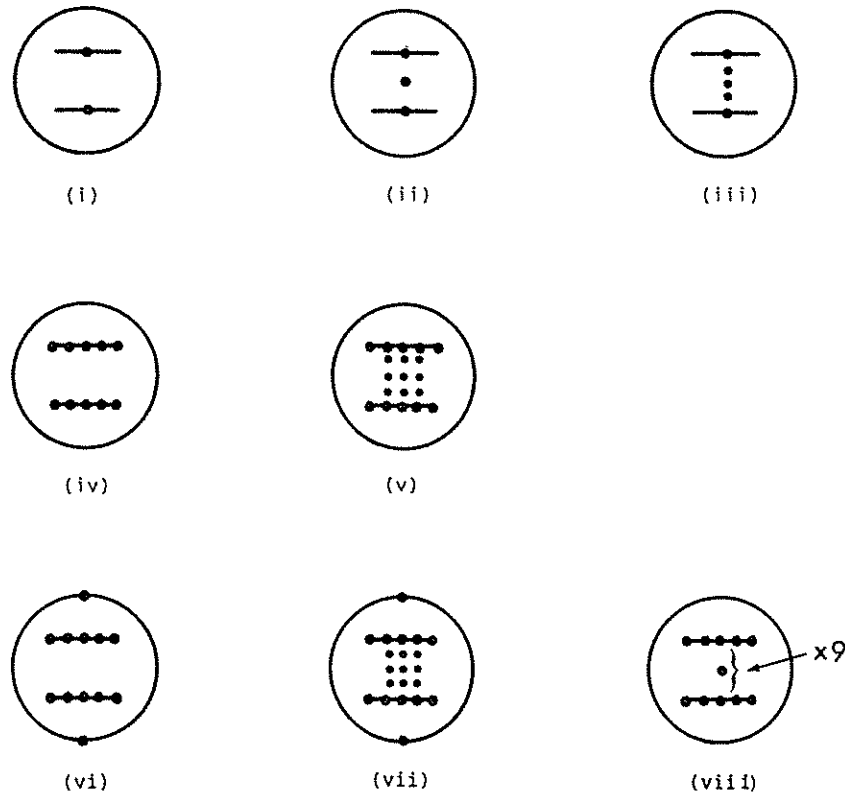


Fig. 5. Combinations of retained degrees of freedom used in validation studies.

of the m free internal nodes in turn, the terms obtained in the successive solution vectors of v_2 represent the columns in the geometric conductance tensor for the disc. This procedure is equivalent to performing the symbolic inversion of equation (12) such that [Zienkiewicz *et al.*, 1977]

$$\begin{Bmatrix} \phi_1 \\ v_2 \end{Bmatrix} = \begin{bmatrix} V_{11} & -\Phi_{12} \\ V_{21} & -\Phi_{22} \end{bmatrix}^{-1} \begin{Bmatrix} -V_{12} & \phi_2 \\ -V_{22} & \phi_2 \end{Bmatrix} \quad (13)$$

and a relationship linking the m discharge velocities v_2 and m nodal potentials ϕ_2 on the internal slits is established. This relationship may be represented in generality as

$$v = A\phi \quad (14)$$

where the matrix A is $m \times m$ in dimension and corresponds to a tensor of geometric conductivity for the fissure disc with all external edge degrees of freedom removed. If the tensor A is premultiplied to relate changes in nodal potential ϕ to nodal discharge q rather than nodal velocities v the matrix statement will correspond directly to finite element format. Premultiplication of the rows of A must be completed by the integrals of the basis functions of equation (3) to yield a . The integrals are of the form

$$a = b \int_{-1}^{+1} h^T \frac{d\Gamma}{d\xi} d\xi \quad (15)$$

where b is the aperture of the fissure. Each row of A is premultiplied by the appropriate nodal terms of equation (15) to yield a tensor K . The geometric conductance tensor directly relates

nodal discharges q to nodal potentials ϕ . Presented in this manner, the relationship

$$q = K\phi \quad (16)$$

is identical to the finite element statement. Although equation (13) derived by this formulation may in general be non-symmetric, the only entries of direct interest in forming A and subsequently K are the basal m rows. Following premultiplication by the integrated shape function terms of a , the K matrix has been observed, in all cases examined to date, to be nominally symmetric. The physical interpretation of this is that a homogeneous system of discharge boundary conditions is applied to a domain truncated by the edge contour. In this instance the coefficient matrix may be expected to be symmetric [Zienkiewicz *et al.*, 1977]. This factor may be explored intuitively by condensing internal nodes to a single degree of freedom for a two-slit disc. Clearly, conservation of mass dictates that the resulting 2×2 matrix is symmetric with the off diagonal terms the negative of the diagonal.

The conductivity tensor K may be considered equivalent to a single multinoded element. Flow within the fissure is controlled only by the boundary conditions applied to the internal nodes. The steady behavior of an assemblage of discs may therefore be determined by assembling the multinoded elements into a global conductance matrix. Conductivity terms for nodes common to multiple discs are merely summed according to usual finite element convention. This results in a positive definite, symmetric, and sparsely populated global matrix. Since the functions of the elemental and global conductance matrices are identical, the global matrix will similarly be referred to in the following as K .

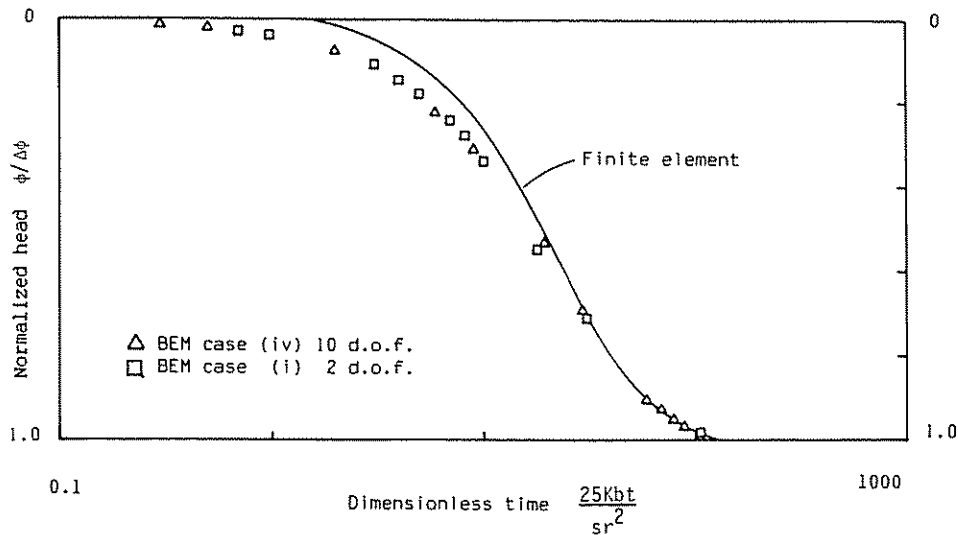


Fig. 6. Normalized transient response of head at slit 2 for finite element and boundary element analysis cases i and iv.

Transient Solution

For a system of interconnected fissures, equation (16) may be assembled from the foregoing and solved for steady state conditions. For transient analysis, the finite element statement at any specific time t is given as

$$\mathbf{K}\phi_t + \mathbf{S}\dot{\phi}_t = \mathbf{q}_t \quad (17)$$

where \mathbf{K} is the same global geometric conductivity tensor defined above, \mathbf{S} is the diagonal matrix of fissure aquifer storativity terms, \mathbf{q}_t is the vector of prescribed nodal discharges at time t , and ϕ_t and $\dot{\phi}_t$ are vectors of nodal hydraulic potentials and time derivatives of potential at time t , respectively.

The elements of the diagonal storativity matrix require that specific storage S_s per unit area and mean aperture for the fissure aquifer b are defined. This, in itself, is not a trivial task as fissure storativity may be shown to be a strongly nonlinear function of effective stress [Elsworth and Goodman, 1985]. In all applications discussed in the following it is assumed that fissure storativity is constant over the range of applied effective stresses [Doe et al., 1982].

The total storativity S for a single fissure disc is defined as

$$S = \int_{\Omega} b \cdot S_s \, d\Omega \quad (18)$$

where the integration is performed over the area of the disc. This integral may be readily evaluated for any simple circular disc or other arbitrary elliptical or rectangular closed domains as required in the above. The only item remaining is to define, in a systematic manner, how the total storativity may be distributed between retained nodal degrees of freedom. Any convenient analysis may be employed whereby a tributary area is ascribed to a single node which will control discharge of that region. Simple division of the domain into tributary units or coarse meshing of finite elements may be used to evaluate the consistent storativity vector \mathbf{S} as

$$\mathbf{S} = b \int_{\Omega} N_i S_s N_j \, d\Omega \quad (19)$$

where N_i and N_j are basis functions for plane elements [Zienkiewicz, 1977]. Coarser coverage of finite elements com-

bined with reduced integration could be used than would be required to accurately define the conductivity of the disc using finite element procedures. This procedure, however, negates one of the main motivations for development of the boundary element technique in this particular application in that internal discretization into elements is not required. In addition, consistent formulations have shown poor performance in transient solution [Neuman and Narasimhan, 1977] and lumped description of storage potential is preferred. For these reasons a simpler procedure is used whereby the total disc storativity is divided between nodes ranked proportionately to the magnitude of the diagonal term in the conductance matrix \mathbf{K} .

Since storativity is lumped only at the retained internal nodes, the magnitude of the terms within the vector \mathbf{S} may be determined from

$$S = \frac{S}{\text{Tr}(\mathbf{K})} [\mathbf{K}] \quad i = j \quad (20)$$

$$S = 0 \quad i \neq j \quad (21)$$

where S is appropriately defined in equation (18). The rationale behind adopting this procedure is that for flow within an isotropic domain the ratio \mathbf{K}/S is retained constant for the matrix identities. This assumption is somewhat arbitrary, although in the light of uncertainty regarding consistent formulation by finite element analysis, it is not considered unrealistic. Any inaccuracies introduced by this assumption may be examined in the light of the validation exercises following. It is apparent, from these results, that the approximation adopted in evaluating \mathbf{S} does not markedly affect precision. This is especially apparent as the number of fissures composing the network is increased. Since this is the ultimate goal of the formulation, this is not considered an overly restrictive requirement.

Implicit Time Integration

The general finite element matrix identity given in equation (17) is exact for any moment in time. If a time step Δt is chosen, equation (17) may be rewritten for time $t + \Delta t$ as

$$\mathbf{K}\phi_{t+\Delta t} + \mathbf{S}\dot{\phi}_{t+\Delta t} = \mathbf{q}_{t+\Delta t} \quad (22)$$

where identities \mathbf{K} and \mathbf{S} remain unchanged. If the variation in

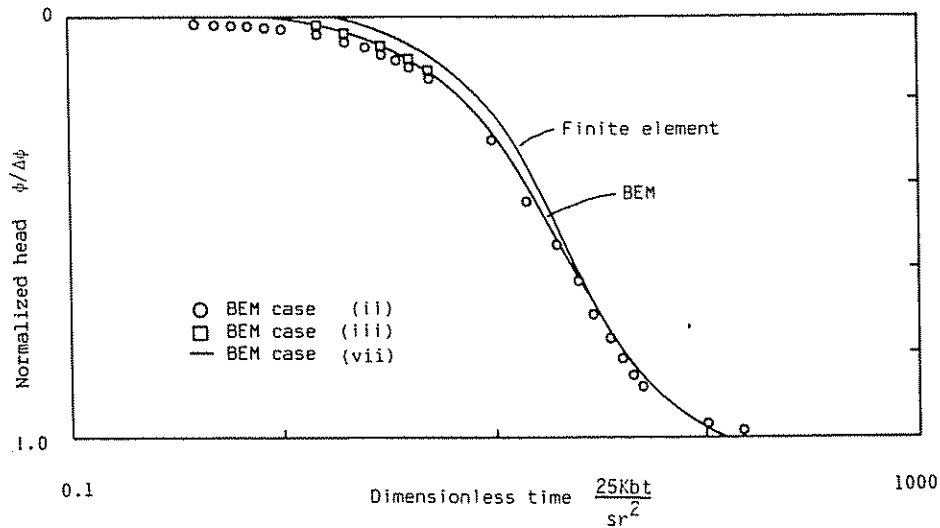


Fig. 7. Normalized transient response of head at slit 2 for finite element and boundary element analysis cases ii, iii, and vii.

nodal hydraulic potential is assumed linear within the incremental time step Δt , then the time derivative of potential may be approximated as

$$\phi_{t+\Delta t} = \frac{1}{\Delta t} (\phi_{t+\Delta t} - \phi_t) \tag{23}$$

which on resubstitution into equation (22) yields for fully implicit application

$$\mathbf{q}_{t+\Delta t}^* = \mathbf{K}^* \phi_{t+\Delta t} \tag{24}$$

where

$$\mathbf{q}_{t+\Delta t}^* = \mathbf{q}_{t+\Delta t} + \frac{S}{\Delta t} \phi_t \tag{25}$$

and

$$\mathbf{K}^* = \mathbf{K} + \frac{S}{\Delta t} \tag{26}$$

Cast in this form, equation (24) may be assembled, triangularized, and used at a suitable incremental time step. Implicit integration in time ensures that time increments of any magnitude may be used with guaranteed stability [Polivka and Wilson, 1976; Neuman and Narasimhan, 1977]. The factored form of \mathbf{K}^* retains the symmetric and sparsely populated nature of the original global matrix of equation (16). Reformation of equation (24) is only required if significant changes in storativity or conductivity of the fissures occur or if it is desired to modify the time increment Δt .

VALIDATION

Validation of the proposed solution procedure is difficult in the absence of an analytical solution for the specific problem geometry. Appropriate validation exercises completed in the following are (1) comparison of the predicted transient response with a finite element representation of a single, circular fissure disc, and (2) comparison of a simple series fissure network with a transient analytical solution.

Circular Fissure Disc

A single circular fissure disc is chosen as the basic subordinate geometric unit comprising a system of fissures. If it is possible to show that the transient performance of a single disc compares favorably with some chosen benchmark, it is reasonable to project that an assembly of discs would produce similarly valid results. In the absence of an analytical standard with which to compare the boundary element solution procedure, a finite element model of identical geometry is used.

A disc diameter to slit length ratio (d/l) of two is chosen for the purpose of validation. The slits are disposed symmetrically about the origin in such a manner as to retain symmetry in both horizontal and vertical sections. The separation between slit centers is equal to the disc radius ($d/2$). The ratio of disc hydraulic transmissivity Kb and storativity S_b is equal to unity. The boundary element and finite element idealizations of the disc geometry are illustrated in Figure 4.

Half symmetry in the finite element model uses 28 nine-noded Lagrangian elements comprising a total of 135 degrees of freedom. The curved elements accurately describe the true form of the fissure edge although, at the chosen density of coverage, this is not of major importance. In the simplest boundary element discretization of the disc a total of eight boundary and four internal slit elements are used. All are three-noded isoparametric elements enabling the curved fissure edge to be accurately represented. This factor is more important for the boundary element discretization given the relatively sparing edge coverage. A total of 26 nodes and corresponding single degrees of freedom exist for the initial system, although this may be condensed down to describe performance purely in terms of the internal nodes. Thus anywhere between a maximum of 10 and a minimum of 2 internal degrees of freedom may be retained for the system.

In addition to performing the analysis with internal nodes located only on the intersection traces with other fissures, additional "virtual" nodes may be set within the body of the disc. This may most simply be achieved if additional internal slit

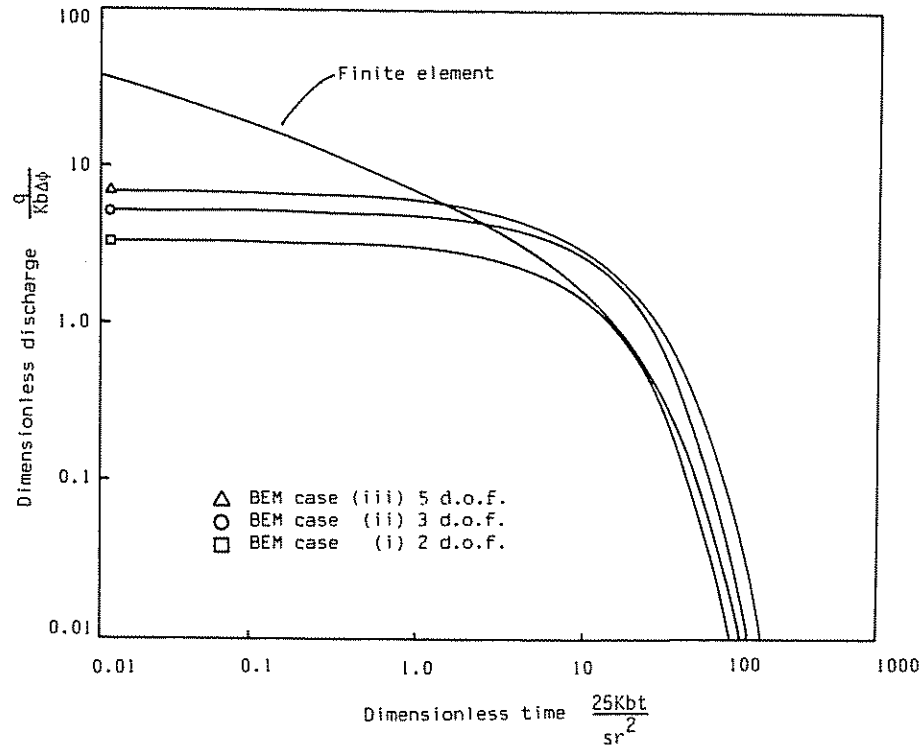


Fig. 8. Transient response of discharge at slit 1 for finite element and boundary element analysis cases i-iii.

elements are dispersed in strategic locations. These “virtual” slits serve to further distribute the storativity of the disc and provide more complete representation of the in-fissure pressure transients. As such, the internal nodes may be useful in enhancing the early hydraulic response of the fissure discs and

thereby optimize the anticipated transient performance. It is timely to mention that although the internal elements mathematically represent slits, they make no longitudinal contribution to flow along their axes. The combinations of retained nodal degrees of freedom used in the following studies are

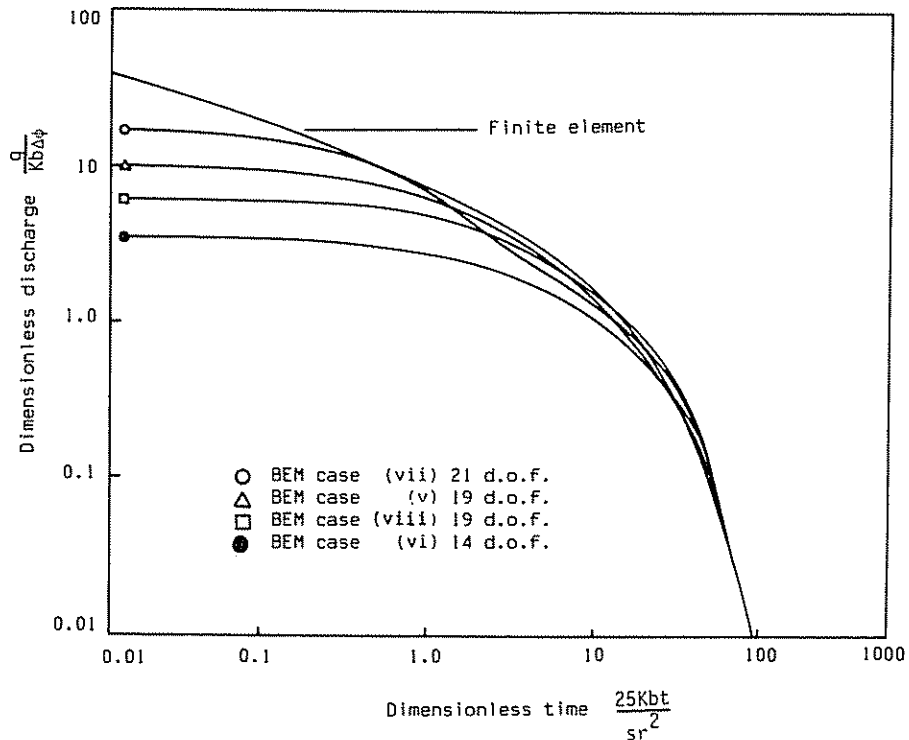


Fig. 9. Transient response of discharge at slit 1 for finite element and boundary element analysis cases v-viii.

illustrated in Figure 5 for a total of eight cases identified sequentially as i-viii. Solid circles denote a single retained degree of freedom.

A single form of hydraulic loading is used in all validation exercises. The distribution of total head within the disc is initially constant and equal to zero ($t = 0^-$). A unit head is applied to slit 1 at time $t = 0^+$, and the variation in hydraulic potential at slit 2 is monitored. Quantitative evaluations of the influent fluid flow at slit 1 and the change in head at slit 2 are two solution parameters available from the boundary element formulation regardless of the number of nodes retained in the system and are therefore used as performance indices.

The transient response of total head at slit 2 is illustrated in Figure 6 where only the internal nodes are retained. With five nodes retained per slit, the length weighted mean of all nodal values is reported in Figure 6. It is evident that little advantage is realized in retaining extra nodes on the individual slits with regard to the transient head response. The difference between the two boundary element solutions exists only at small dimensionless times. There appears, however, to be a discrepancy between the boundary element and finite element simulations in this initial period. The magnitude of the offset may be acceptable, however, depending on the particular application.

If single or triple "virtual" nodes are added to the configuration (cases ii and iii), the solution accuracy improves slightly, as illustrated in Figure 7. Further improvement is possible if extra internal and edge nodes are utilized. A total of nine internal and two edge nodes are used in case vii with the results similarly illustrated in Figure 7. It is important to note that only a relatively small improvement in response is attained for a drastic increase in the number of retained and generated degrees of freedom. Using triple "virtual" nodes, five degrees of freedom are retained; in case vii a total of 21 degrees of freedom are retained.

Transient discharges evaluated at the sole exit from the fissure disc are illustrated in Figures 8 and 9 for different

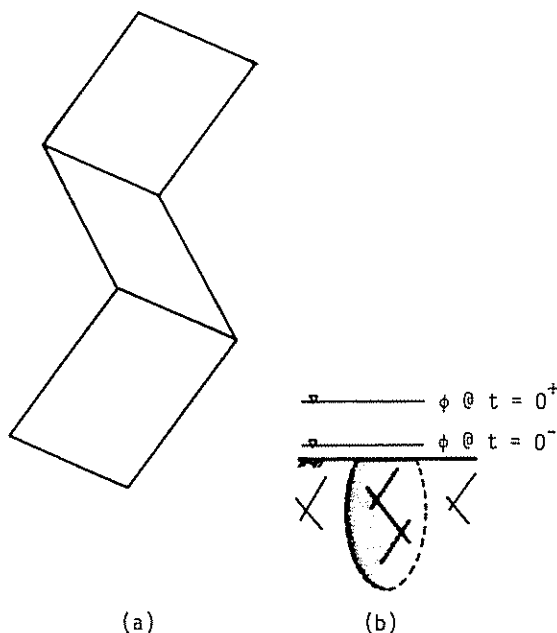


Fig. 10. Perspective view of (a) a three-dimensional series fissure network and (b) corresponding hydraulic loading sequence.

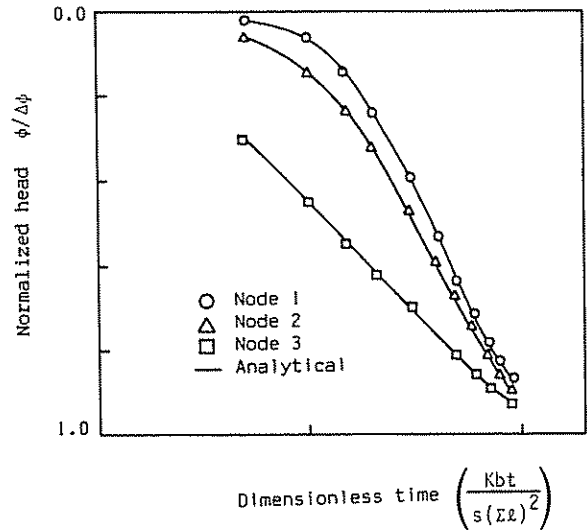


Fig. 11. Transient response of the series fissure system. Analytical versus numerical characterizations.

nodal and elemental densities. Log-log plots of dimensionless discharge and dimensionless time are used to present response over four log cycles of time. Where only a single degree of freedom is retained per slit, results are presented in Figure 8. The geometry without "virtual" nodes exhibits poor performance at small dimensionless times, but very good agreement is attained with the finite element control at large dimensionless times. Where additional virtual nodes are incorporated into the disc geometry as in cases ii and iii, the early time performance is improved, however, to the detriment of the long-term performance. It is believed that this paradox results from the presence of stored fluid, present within the system, that is available for discharge at large dimensionless times having not been transmitted previously. It is likely that requiring a major portion of the fissure storage to be located between the slits prevents the portion of the fissure close to the edge from draining effectively in the short term. Thus initial drainage is deficient with the net result that a great deal of storage is available for depletion as the transient disturbance reaches progressively further outward. The ability of the disc to discharge this fluid early is enhanced over the 2 degrees of freedom case due to more accurate transient representation of internal heads and hydraulic gradients. The magnitude of the initial gradient at $t = 0^+$ is controlled by the separation of slit 1 and the closest "virtual" node. The effect of this is clearly illustrated in the early system responses of Figure 8, where "virtual" nodes located progressively closer to the disturbed slit yield better approximations of the early discharge. Numerical singularity considerations provide a threshold limit of separation, however, closer than which adjacent nodes should not be located.

The transient responses for discretization cases v-viii are illustrated in Figure 9. It is evident that retaining all five slit nodes for solution and adding four boundary nodes as in case vi does not improve accuracy over the case of a 2 degrees of freedom disc (case i). Successive addition of internal nodes, as illustrated in Figure 9, considerably benefits the early response with no detrimental effects in the long term. For discretization case vii, no adverse effect on the response was observed where the slits are represented by a single degree of freedom with the remaining edge and internal nodes retained. This performance

is encouraging in that it represents a total of only 13 unknowns.

Rectangular Fissure Model

Since the behavior of a single fissure disc will represent only one component of the complete fracture network, it is appropriate to evaluate the ramifications of the previous validation studies in a global context. It does not necessarily follow that any deficiencies encountered in representing the transient behavior of a single fissure will be evident either to the same degree or even at all in the global network. It is important therefore to evaluate rigorously the performance of the network, where possible, against analytical solution.

The geometry of a simple three-fissure network is illustrated in Figure 10. For the case where fissure intersections provide no additional friction loss, the transient response of the four-noded system is directly analogous to heat conduction within an infinite plate, cooled from an ambient temperature on one surface and perfectly insulated on the other surface [Terzaghi, 1943]. A parallel is drawn in this work where the change in system pressure head is monitored with time. A comparison between the analytical and assembled boundary element solutions is illustrated in Figure 11. Each rectangular fissure of aspect ratio equal to unity is represented externally by eight elements and 16 nodes. The individual fissures are condensed to 2 degrees of freedom, one at each end. Excellent correspondence between the analytical and numerical results is achieved even for the extremely sparse coverage of only three fissures.

CONCLUSIONS

A numerical method is presented to evaluate the transient response of discretely fractured systems in a systematic and computationally economic manner. All reductions for the boundary procedure are at the elemental or individual disc level prior to global network assembly. Cast in this form, the solution technique is ideally suited to preprocessing by mini-computer to reduce the number of disc degrees of freedom to a desired minimum level. With this initial reduction completed at the disc level, global assembly may be completed by file uploading to a machine of larger capacity. The initial reduction procedure is especially expedient for transient analysis where multiple time-stepping iterations will be completed. The traditional advantages of boundary element solution, namely, ease of data input and systematic element generation, are retained. Although developed with specific reference to circular discs, the solution method may accommodate fissures of any arbitrary edge contour if field data merit their inclusion. The resulting global matrices are, for all cases run to date, well conditioned, sparsely populated, symmetric, and, for all fully connected networks, positive definite.

The performance of both individual fissures and assembled fissure networks is illustrated to be satisfactory. The early response of individual units is shown to be strongly dependent on the number of internal and edge nodes retained for the global analysis. Extra nodes retained on the individual fissure slits apparently offer little advantage in accuracy and penalize solution computational economy.

Although the early transient response is lacking for relatively sparing nodal coverage of an individual disc, this factor will be critical only if gauging the early response is important or, alternately, if the early response markedly affects the long-term response. The true importance of this apparent deficiency in the analysis procedure may only be determined for each specific application by the individual user. It appears, how-

ever, from the validation studies that the short-term performance does not adversely affect the long-term response. In this vein the performance of a simple four-noded network is illustrated to perform very well. Thus the previously imposed constraint that an individual disc must perform exceptionally well to guarantee performance fidelity of an assemblage may well be overdemanding. It appears from the case illustrated in Figure 11 that the poor early performance aspects of the method are apparent neither at relatively large dimensionless times or for fissure networks containing multiple units. The validity of this observation may only be compared against future numerical or physical studies.

NOTATION

A	disc geometric conductivity matrix with respect to velocities.
K, K, K^*	fissure hydraulic conductivity, disc geometric hydraulic conductivity tensor with respect to discharge, and modified tensor, respectively.
M	unit source strength.
N_i	element basis function.
S_s, S, S	specific storage, storativity, and diagonal storativity matrix, respectively.
$V(i, j), \Phi(i, j)$	kernel functions for a unit source.
V, Φ	matrices containing integrated kernel functions.
a	premultiplication factor to convert nodal velocity into nodal discharge.
b	fissure aperture.
$c(i)$	free term.
d	disc diameter.
h^T	vector of element shape functions.
l	fissure intersection slit length.
\bar{n}	domain unit outer normal.
i	location of unit line or point source.
j	location of point of interest.
q, q^*	vector of prescribed nodal discharges, modified vector.
r	radius i to j .
$t, \Delta t$	time, increment of time.
$v(j), v$	nodal velocity, vector of nodal velocities normal to the boundary.
w_i	integration weight.
x, y	Cartesian coordinate system.
$\phi(j), \phi, \phi$	nodal hydraulic head, vector of nodal heads, vector of time derivatives of nodal heads.
δ_{ij}	Kronecker delta $\delta_{ij} = 1, i = j; \delta_{ij} = 0, i \neq j$.
Ω	domain.
Γ	domain boundary.
ξ, η	intrinsic coordinates for isoparametric element.

Acknowledgments. This work was supported by the Pennsylvania Mining and Mineral Resources Research Institute under grant 91154142 from the Bureau of Mines, U.S. Department of the Interior. Review of the manuscript and constructive criticism by Richard R. Parizek is most warmly appreciated.

REFERENCES

- Anderson, D. G., Gaussian quadrature formulae for $\int \ln(x)f(x) dx$, *Math. Comput.*, 19, 477-481, 1965.
- Banerjee, P. K., and R. Butterfield, *Boundary Element Methods in Engineering Science*, McGraw-Hill, New York, 1981.
- Barenblatt, G. I., Yu. P. Zheltov and I. N. Kochina, Basic concepts in the theory of seepage of homogeneous fluids in fissured rocks, *J. Appl. Math. Mech.*, 24, 1286-1303, 1960.
- Doe, T. W., J. C. S. Long, H. K. Endo, and C. R. Wilson, Approaches to evaluating the permeability and porosity of fractured rock

- masses, *Proc. U.S. Symp. Rock Mech.* 23rd, 30-38, 1982.
- Elsworth, D., A hybrid boundary element-finite element analysis procedure for fluid flow simulation in fractured rock masses, *Int. J. Numer. Anal. Methods Geomech.*, in press, 1986.
- Elsworth, D., and R. E. Goodman, Hydro-mechanical characterisation of rock fissures of idealised sawtooth or sinusoidal form, paper presented at Symposium on Fundamentals of Rock Joints, Int. Soc. for Rock Mech., Björkliden, Sweden, 1985.
- Elsworth, D., and R. E. Goodman, Characterisation of rock fissure hydraulic conductivity using idealised wall roughness profiles, *Int. J. Rock Mech. Min. Sci. Geomech. Abstr.*, 23(3), 233-244, 1986.
- Jaswon, H. A., Integral equation methods in potential theory, I, *Proc. R. Soc. London, Ser. A*, 275, 33-46, 1963.
- Kellog, O. D., *Foundations of Potential Theory*, Dover, Mineola, N.Y., 1953.
- Long, J. C. S., Investigation of equivalent porous medium permeability in networks of discontinuous fractures, Ph.D. thesis, Univ. of Calif., Berkeley, 1983.
- Long, J. C. S., and P. A. Witherspoon, The relationship of the degree of interconnection to permeability in fracture networks, *J. Geophys. Res.*, 90(B4), 3087-3098, 1985.
- Long, J. C. S., P. Gilmour, and P. A. Witherspoon, A model for steady fluid flow in random three-dimensional networks of disc-shaped fractures, *Water Resour. Res.*, 21(8), 1105-1115, 1985.
- Neuman, S. P., and T. N. Narasimhan, Mixed explicit-implicit iterative finite element scheme for diffusion-type problems, I, Theory, *Int. J. Numer. Methods Eng.*, 11, 309-323, 1977.
- Noorishad, J., M. S. Ayatollahi, and P. A. Witherspoon, A finite-element method for coupled stress and fluid flow analysis in fractured rock masses, *Int. J. Rock. Mech. Min. Sci. Geomech.*, 19, 185-193, 1982.
- Polivka, R. M., and E. L. Wilson, Finite element analysis of nonlinear heat transfer problems, *Rep. UC SESM 76-2*, Dep. of Civ. Eng., Univ. of Calif., Berkeley, 1976.
- Sagar, B., and A. Runchal, Permeability of fractured rock: Effect of fracture size and data uncertainties, *Water Resour. Res.*, 18(2), 266-274, 1982.
- Shapiro, A. M., and J. Andersson, Steady state fluid response in fractured rock: A boundary element solution for a discrete fracture continuum model, *Water Resour. Res.*, 19(4), 959-969, 1983.
- Snow, D. T., A parallel plate model of fractured permeable media, Ph.D. thesis, Univ. of Calif., Berkeley, 1966.
- Stroud, A. H., and D. Secrest, *Gaussian Quadrature Formulas*, Prentice-Hall, Englewood Cliffs, N.J., 1966.
- Symm, G. T., Integral equation methods in potential theory, II, *Proc. R. Soc. London, Ser. A*, 33-46, 1963.
- Terzaghi, K., *Theoretical Soil Mechanics*, John Wiley, New York, 1943.
- Wilson, C. R., and P. A. Witherspoon, Steady state flow in rigid networks of fractures, *Water Resour. Res.*, 10(2), 328-335, 1974.
- Zienkiewicz, O. C., *The Finite Element Method*, 3rd ed., McGraw-Hill, New York, 1977.
- Zienkiewicz, O. C., D. W. Kelly, and P. Bettes, The coupling of the finite element method and boundary solution procedures, *Int. J. Numer. Methods Eng.*, 11, 355-375, 1977.

D. Elsworth, Department of Mineral Engineering, 104 Mineral Sciences Building, Pennsylvania State University, University Park, PA 16802.

(Received August 16, 1985;
revised July 31, 1986;
accepted August 1, 1986.)

